Thai Journal of Physics Vol. 38 No. 2 (2021) 69-98

Original Research Article

Geodesic Dynamics in Reissner-Nordström Geometry

Daniel Abramson*

9/72 Soi Kasemsan 3, Rama 1 Road, Wangmai, Pathumwan, Bangkok 10330

*Corresponding author E-mail: khunchang@gmail.com

Received: 28th May 2021, Revised: 22nd July 2021, Accepted: 24th July 2021

Abstract

We analyze geodesics (trajectories of free-falling bodies) in the geometry created by a Reissner-Nordström black hole. Bound and unbound radial orbits are obtained first in the superextremal case, then in the extremal and subextremal cases where geodesics penetrate a horizon, inside of which an outside observer cannot see. We determine the location of geodesics in conformal (Penrose) spacetime diagrams. We also deduce that the "river model", a useful idea to explain the behavior of Schwarzschild black holes, fails in the case where electric charge is present.

Keywords: Reissner-Nordström, Black hole, Geodesic, Penrose diagram

Introduction

The solution of Einstein's field equations for a spherically symmetric mass distribution was found by Karl Schwarzschild in 1916 [1], leading to the theoretical possibility of black holes. The spacetime geometry created by a static, non-rotating black hole with mass m and electric charge q was determined independently by Hans Reissner in 1916 [2] and Gunnar Nordström in 1918 [3].[1,2] The geometry created by such a charged black hole is determined by the metric

$$ds^2 = -\left(1 - \frac{2m}{r} + \frac{q^2}{r^2}\right)dt^2 + \frac{dr^2}{1 - 2m/r + q^2/r^2} + r^2 d\theta^2 + (r\sin\theta)^2 d\phi^2 \,.$$

[1] Geometrized units where $G = c = 1$ are used in this paper, so that mass and charge have units of length. These quantities can be converted to units of length by multiplying by the conversion factors

$$G/c^2 = 7.43 \times 10^{-28}\,\mathrm{m/kg}$$

$$\sqrt{G/4\pi\epsilon_0 c^4} = 8.62 \times 10^{-18}\,\mathrm{m/C}$$

[2] We investigate only the case of static (eternal), spherically symmetric, non-rotating black holes. Black holes created at a finite prior time (by stellar collapse or some other means) are not considered.

This is not a vacuum solution since the geometry is determined by both the mass and the electric field with energy density $\mathbf{E}^2/8\pi = q^2/8\pi r^4$.

Reissner-Nordström black holes receive cursory treatments in the text literature [4,5] or are introduced as exercises [6,7]. This can be attributed to circumstances and hypotheses which suggest that the phenomena associated with charged black holes are likely to be unphysical.[3] Notwithstanding this, the Reissner-Nordström solution has intrinsic interest and shares features of the Kerr solution for rotating black holes.

Useful Formulas and Identities

We establish several elementary results which will be used repeatedly.

A. Notation

$d\tau_g$ denotes proper time along a *geodesic*. When there is no possibility of confusion, we will write $d\tau$.
$d\tau_r$ denotes proper time for a stationary ***shell observer*** $\mathcal{S}_r$ located at radius r.
A dot ⬚ always denotes differentiation with respect to proper time along a geodesic: $\dot{r} \equiv dr/d\tau_g$.

B. Shell observer speed

We consider metrics of the form

$$ds^2 = -f(r)\,dt^2 + \frac{dr^2}{f(r)} + r^2 d\theta^2 + (r\sin\theta)^2 d\phi^2\,. \tag{1}$$

We assume $f(\infty) = 1$, so the spacetime geometry is asymptotically flat. In the case of radial motion $(d\theta = d\phi = 0)$ the metric simplifies to

$$ds^2 = -f(r)\,dt^2 + \frac{dr^2}{f(r)}.$$

A shell observer $\mathcal{S}_r$, who is stationary on the sphere of radius r, measures the speed of an object in (timelike) motion in his frame of reference:

$$v_r = \frac{\text{proper length}}{\text{proper time}} = \frac{ds\big|_{dt=0}}{\sqrt{-ds^2}\big|_{d\mathbf{x}=0}}.$$

[3] Such as the cosmic censorship conjecture, mass inflation instability, and the sheer amount of excess charge needed for the inner event horizon radius to reach the Compton wavelength of an elementary particle or even the Planck length.

Therefore

$$v_r^2 = \frac{dr^2/f(r)}{f(r)\,dt^2} = \frac{dr^2/dt^2}{f(r)^2} \quad \Longrightarrow \quad v_r = \frac{1}{f(r)}\frac{dr}{dt}. \tag{2}$$

We choose the positive square root in (2) so that v_r has the same sign as dr/dt when $f(r) > 0$.[4]

The proper time element $d\tau_r$ for a shell observer $\mathcal{S}_r$ is

$$d\tau_r = \sqrt{-ds^2}\Big|_{d\mathbf{x}=0} = \sqrt{f(r)}\,dt\,. \tag{3}$$

Therefore, by (2) and (3):

$$v_r = \frac{1}{f(r)}\frac{dr}{dt} = \frac{1}{f(r)}\frac{dr}{d\tau_g}\frac{d\tau_g}{d\tau_r}\frac{d\tau_r}{dt} = \frac{\dot{r}\sqrt{1-v_r^2}\sqrt{f(r)}}{f(r)} = \frac{\dot{r}\sqrt{1-v_r^2}}{\sqrt{f(r)}}.$$

Solving for v_r^2:

$$v_r^2 = \frac{\dot{r}^2}{f(r)+\dot{r}^2}\,. \tag{4}$$

It follows that $|v_r| < 1$ if and only if $f(r) > 0$.

C. Geodesic motion

Timelike geodesic trajectories in the equatorial plane $\theta = \pi/2$ satisfy the equations of motion:[5]

$$\begin{aligned} \dot{\phi} &= \frac{\ell}{r^2} \\ \dot{t} &= \frac{e}{f(r)} \\ \dot{r}^2 &= e^2 - \left(1 + \frac{\ell^2}{r^2}\right) f(r) \end{aligned} \tag{5}$$

[4] $f(r) < 0$ corresponds to a black or white hole; see (37) and Figure 13. Along a timelike path in such a region, dr never changes sign — $dr < 0$ in a black hole — but dt can be positive, negative or zero. Thus "ingoing" objects $(dr/dt < 0)$ and "outgoing" objects $(dr/dt > 0)$ both move in the direction of decreasing r.

[5] A straightforward generalization of the derivation given by Dray [8] (pp. 21-23) for Schwarzschild geometry.

where e and ℓ are constants of the motion.[6] For a geodesic that starts from rest at infinity, the third equation in (5) shows that $e^2 = f(\infty) = 1$.

For a radial geodesic, $\dot{\phi} = 0$ implies $\ell = 0$, whence $\dot{r}^2 = e^2 - f(r)$. Inserting this into (4) yields two useful relations (taking $e > 0$):

$$v_r = \frac{\dot{r}}{e} \tag{6}$$

$$v_r = 1 - \frac{f(r)}{e^2} \tag{7}$$

From (7) we may deduce that e is the ratio of total energy E to mass M of a free-falling object measured by a distant, stationary observer.[7] We verify this as follows. In a potential energy field U the total energy is $E = \gamma M + U$, where $\gamma = (1 - v^2)^{-1/2}$ and U are both functions of position. Hence:

$$\left(\frac{M}{E-U}\right)^2 = \left(\frac{1}{\gamma}\right)^2 = 1 - v^2 = 1 - \left(1 - \frac{f(r)}{e^2}\right) = \frac{f(r)}{e^2}.$$

Thus $(E-U)/M = e/\sqrt{f(r)}$. Letting $r \to \infty$ we obtain $E/M = e$.

Henceforth all geodesics will henceforth be assumed to be radial.

Preliminaries

The Reissner-Nordström metric is given by (1) with

$$f(r) = 1 - \frac{2m}{r} + \frac{q^2}{r^2} = 1 - \frac{2m(r-\beta)}{r^2} \tag{8}$$

where $\beta \equiv q^2/2m$. The radial equation of motion along a geodesic is given by (5):

$$\dot{r}^2 = e^2 - \left(1 - \frac{2m(r-\beta)}{r^2}\right). \tag{9}$$

For an object that starts from rest at infinity, $e = 1$, so its equation of motion is

$$\dot{r}^2 = \frac{2m(r-\beta)}{r^2}. \tag{10}$$

[6] ℓ is the angular momentum per unit mass.

[7] All test "objects" are assumed to be uncharged, and therefore do not interact with the electric field.

Since the trajectory is ingoing, we conclude:

$$\dot{r} = -\frac{\sqrt{2m(r-\beta)}}{r}. \tag{11}$$

We see that the object comes to a stop at $r = \beta$ and moves no closer to the singularity.

A shell observer $\mathcal{S}_r$ measures the object's speed from (6):

$$v_r = \frac{\dot{r}}{e} = -\frac{\sqrt{2m(r-\beta)}}{r} \tag{12}$$

Since a shell observer cannot observe an object with nonzero mass traveling with speed $|v_r| \geq 1$, it must be that

$$\frac{2m(r-\beta)}{r^2} < 1 \quad \Leftrightarrow \quad 0 < 1 - \frac{2m(r-\beta)}{r^2} = f(r) \quad \Leftrightarrow \quad P(r) = r^2 - 2mr + q^2 > 0\,.$$

$P(r)$ has discriminant $4(m^2 - q^2)$, so there are three distinct scenarios:

(i) If $|q| > m$, then $P(r)$ has no real zeros and $|v_r| < 1$ for all r. This is a ***superextremal*** singularity.

(ii) If $|q| < m$, then $P(r) = 0$ at $r_\pm = m \pm \sqrt{m^2 - q^2}$. In the region $r_- < r < r_+$ we find $f(r) < 0$. In this region $|v_r| > 1$ so no shell observers can exist. The radii r_- and r_+ are the ***inner*** and ***outer event horizons***. This case is called ***subextremal***.

(iii) If $|q| = m$, then $P(r) = 0$ at $r = m$. There is only a single horizon, which separates regions where $P(r) > 0$. This case is called ***extremal***.

We consider these cases separately.

Superextremal Singularities

A. Geodesics originating from $r = \infty$

In the superextremal case, $f(r) > 0$ for all r, so by (4) we have $|v_r| < 1$ for all $\beta \leq r < \infty$. This is apparent in Figure 1, which shows v_r given by (12) for various values of q. The curves for $q > m = 1$ correspond to superextremal singularities; the other curves will be referenced later.

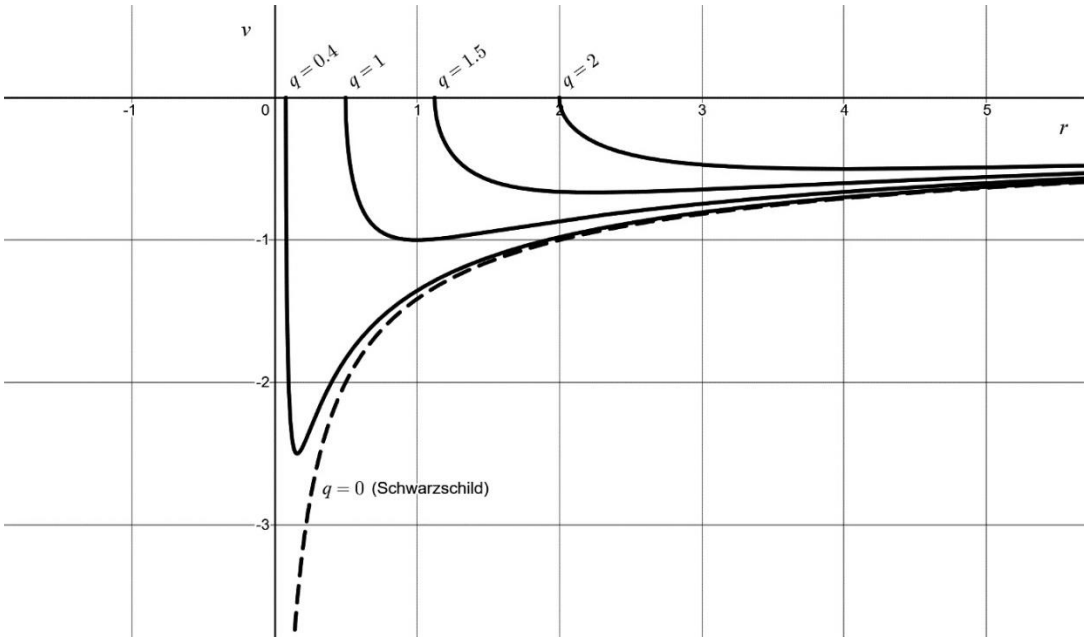

Figure 1 Shell-observer speed v_r for a free-falling object starting from rest at infinity. $q > 0$ is Reissner-Nordström geometry; $q = 0$ is Schwarzschild geometry. $q > m$ $(m = 1)$ corresponds to a superextremal singularity.[8]

The trajectory is obtained by integrating

$$\dot{r} = \frac{dr}{d\tau} = -\frac{\sqrt{2m(r-\beta)}}{r} \tag{13}$$

to obtain

$$\tau = \int \frac{-r dr}{\sqrt{2m(r-\beta)}} = -\left(\frac{2}{9m}\right)^{\frac{1}{2}} \sqrt{r-\beta}\,(r+2\beta) + C\,. \tag{14}$$

Choosing $C = 0$ is equivalent to the condition $r = \beta$ at $\tau = 0$. Eqn. (14) can be inverted to obtain the trajectory $r(\tau)$.

Free fall times. A freely falling object starting from rest at infinity falls from $r = R$ to $r = \beta$ in finite proper time:

$$\Delta\tau = \left(\frac{2}{9m}\right)^{\frac{1}{2}} \sqrt{R-\beta}\,(R+2\beta)\,. \tag{15}$$

[8] We choose $m = 1$ in all figures in this paper.

The time to fall from R to β measured by a far-away observer (or a shell observer) is also finite. By (2):

$$\frac{dr}{dt} = f(r)v_r = -\frac{(r^2 - 2m[r-\beta])\sqrt{2m(r-\beta)}}{r^3}$$

so

$$\Delta t = \int_{\beta}^{R} \frac{r^3 dr}{(r^2 - 2m[r-\beta])\sqrt{2m(r-\beta)}}.$$

This integral can be evaluated in elementary functions but is messy. When r is close to β the integrand is $\approx \beta/\sqrt{2m(r-\beta)}$ which is integrable over an interval $\beta < r < \beta + \varepsilon$. Hence, $\Delta t < \infty$.

To find $\Delta\tau_r$ we use (2) and (3) to obtain

$$\frac{dr}{d\tau_r} = \frac{dr}{dt}\frac{dt}{d\tau_r} = \sqrt{f(r)}\, v_r$$

so that

$$\Delta\tau_r = \int_{\beta}^{R} \frac{r^2 dr}{\sqrt{r^2 - 2m(r-\beta)}\sqrt{2m(r-\beta)}} < \infty .$$

B. Dynamics at $r = \beta$

Once an object that falls from infinity comes to rest at $r = \beta$ (or assuming an object starts from rest at $r = \beta$), the equation of motion is given by (10); however, the direction of motion is now outgoing. To verify this, differentiate (10):

$$2\dot{r}\ddot{r} = \frac{2m(2\beta - r)\dot{r}}{r^3} . \tag{16}$$

At $r = \beta$ we have $\dot{r} = 0$, so (16) is not informative. However, since $\dot{r} \neq 0$ for all $r \neq \beta$, we let $r \to \beta$ to deduce that $\ddot{r}(\beta) = m/\beta^2 > 0$. Therefore, the object is accelerating outward at $r = \beta$ (the singularity is repulsive).[9] Therefore, the equation of motion is given by (10) with the positive square root:

$$\dot{r} = \frac{\sqrt{2m(r-\beta)}}{r} . \tag{17}$$

[9] This refers to the spatial acceleration $\ddot{r}$. The four-acceleration $\ddot{\mathbf{X}} = \mathbf{0}$ on a geodesic.

The trajectory is just the reverse of the ingoing geodesic (14):

$$\tau = \int \frac{rdr}{\sqrt{2m(r-\beta)}} = \left(\frac{2}{9m}\right)^{\frac{1}{2}} \sqrt{r-\beta}(r+2\beta) + C \tag{18}$$

and has the asymptotic behaviors:

$$r \approx \beta: \quad \dot{r} \approx \frac{\sqrt{2m(r-\beta)}}{\beta} \quad \Longrightarrow \quad r(\tau) \approx \frac{m\tau^2}{2\beta^2} + \beta$$

$$r \gg \beta: \quad \dot{r} \approx \sqrt{\frac{2m}{r}} \quad \Longrightarrow \quad r(\tau) \approx \left(\frac{9m}{2}\right)^{\frac{1}{3}} \tau^{2/3} \tag{19}$$

Figure 2 shows joined-up ingoing and outgoing trajectories for various values of q.

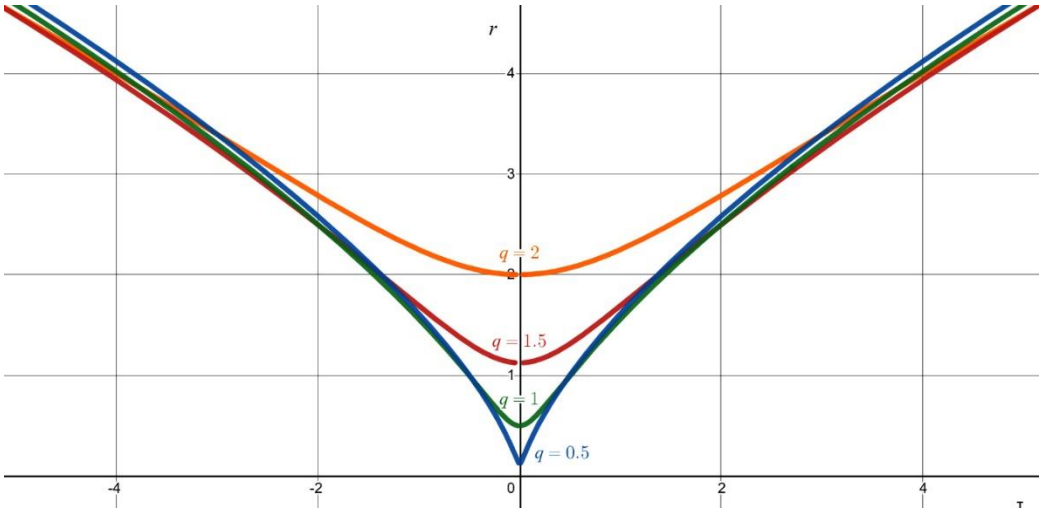

Figure 2 Trajectory $r(\tau)$ of a geodesic starting from rest at infinity, for $q = 0.5, 1, 1.5, 2$.

C. Geodesics starting from $r = \rho > \beta$

Suppose an object starts from rest at radius $\rho > \beta$. From (9):

$$e^2 = 1 - \frac{2m(\rho-\beta)}{\rho^2}$$

so the equation of motion is

$$\dot{r}^2 = \frac{2m(r-\beta)}{r^2} - \frac{2m(\rho-\beta)}{\rho^2} = -\frac{2m(\rho-\beta)}{\rho^2 r^2}(r-\rho)\left(r - \frac{\rho\beta}{\rho-\beta}\right)$$

$$= -\frac{2m(\rho-\beta)}{\rho^2 r^2}(r-\rho)(r-\omega) \tag{20}$$

where $\omega \equiv \rho\beta/(\rho-\beta)$.

The variables ρ and ω and their properties. Note that $\dot{r}$ vanishes at $r=\rho$ and $r=\omega$. Solutions to (20) exist under the following conditions:

(i) $\rho > \beta$: when r lies in the interval between ρ and ω.

(ii) $\rho = \beta$: when $r \geq \beta$.

(iii) $\rho < \beta$: when $r \geq \rho$ (since $\omega < 0$).

Only case (i) interests us now. Case (ii) has already been solved, and case (iii) will be examined later. Note that $\rho\omega = (\rho+\omega)\beta$, which represents a conjugacy between ρ and ω. We record some useful identifies for later use:

$$\begin{aligned} \rho\omega &= (\rho+\omega)\beta \\ \frac{\rho^2}{\rho-\beta} &= \frac{\rho\omega}{\beta} = \rho+\omega \\ \frac{\rho\beta}{\omega} &= \rho-\beta \end{aligned} \tag{21}$$

Using the second identity in (21) we can rewrite the equation of motion (20):

$$\dot{r}^2 = \left(-\frac{2m}{\rho+\omega}\right)\frac{(r-\rho)(r-\omega)}{r^2} \tag{22}$$

The following relationships will be useful to observe (see Figure 3):

If $2\beta < \rho$ then $\beta < \omega < 2\beta$ (in particular, $\omega < \rho$)

If $\rho = 2\beta$ then $\omega = \rho$

If $\beta < \rho < 2\beta$ then $2\beta < \omega$ (in particular, $\rho < \omega$)

If $0 < \rho < \beta$ then $\omega < 0$, $\rho + \omega < 0$, and $|\omega| > \rho$ (23)

Note that:

$\rho \to \infty \implies \omega \downarrow \beta$ (the geodesic that starts from rest at infinity)

$\rho \downarrow \beta \implies \omega \to \infty$ (the geodesic that starts from rest at $r=\beta$)

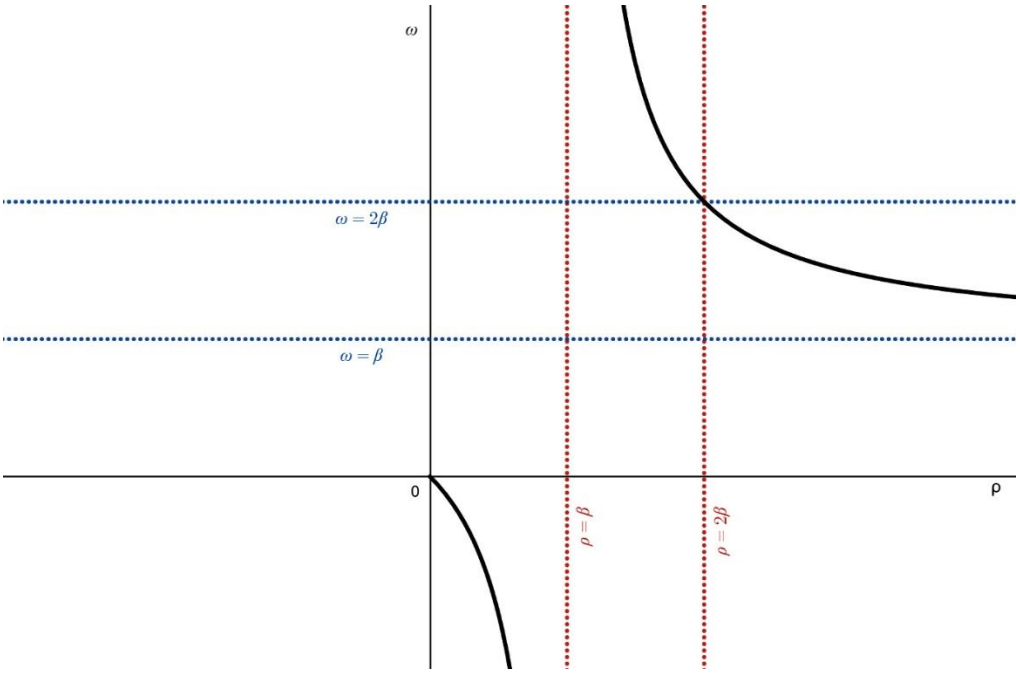

Figure 3 Relationship between ρ *and* $\omega(\rho) = \rho\beta/(\rho - \beta)$.

Trajectory starting from ρ. In which direction does the object begin to move from $r = \rho$? Differentiating (20) with respect to τ gives (16) again. As before, we need to be a little careful since $\dot{r} = 0$ at ρ, the starting point. Since $\dot{r}$ vanishes only at ρ and ω, we can let $r \to \rho$ to deduce that $\ddot{r}(\rho) = m(2\beta - \rho)/\rho^3$. Hence

$$\ddot{r} = \frac{m(2\beta - r)}{r^3} \tag{24}$$

is valid for all $r > 0$. Therefore:[10]

(i) If $\rho > 2\beta$, the motion is *ingoing*, since $\ddot{r} < 0$ (which agrees with $\omega < \rho$).

(ii) If $\beta < \rho < 2\beta$, the motion is *outgoing*, since $\ddot{r} > 0$ (which agrees with $\rho < \omega$).

(iii) If $\rho = 2\beta$, there is *no motion* ($\dot{r} = \text{constant} = 0$), since $\ddot{r} = 0$ (which agrees with $\omega = \rho$).

The object therefore travels in a periodic orbit between $r = \rho$ and $r = \omega$. Figure 4 shows $\dot{r}$ plotted against r for various values of $\rho > 2\beta$. The black trajectory is the ingoing geodesic starting at ρ and ending at ω. The green plot is the outgoing geodesic starting at ρ and ending at ω. For $\beta < \rho < 2\beta$ the orbits are the same with ρ and ω reversed.

[10] We will see that in the subextremal case, $r = 2\beta$ lies in a black hole region where $\dot{r} < 0$. Hence the initial condition $\dot{r}(\rho) = 0$ does not apply in this case.

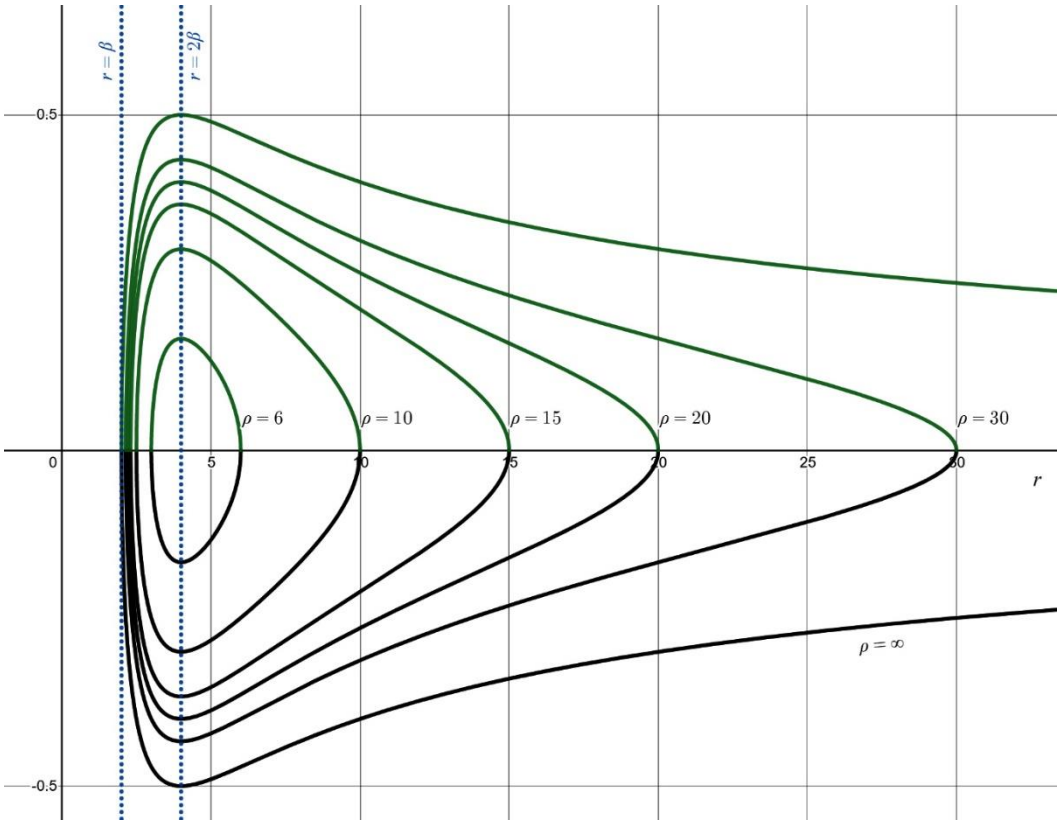

Figure 4 Radial speed $\dot{r}$ (vertical axis) for geodesic trajectories starting from rest at $\rho = 6, 10, 15, 20, 30, \infty$ $(\beta = 2)$.

The equation of motion (22) can be integrated to obtain the trajectory:

$$\tau = \int \frac{dr}{\dot{r}} = \pm\sqrt{\frac{\rho+\omega}{2m}} \int \frac{r dr}{\sqrt{(\rho - r)(r - \omega)}}. \tag{25}$$

The integral in (25) can be evaluated explicitly:

$$\tau = \pm\sqrt{\frac{\rho+\omega}{2m}} \left\{ \sqrt{(\rho - r)(r - \omega)} + \left[\frac{\rho+\omega}{2}\right] \arcsin\left(\frac{\rho + \omega - 2r}{\rho - \omega}\right) \right\} + C \tag{26}$$

and inverted to obtain $r(\tau)$.

Figure 5 shows part of an orbit given by (26) with outer turning point $\rho = 6$ and inner turning point $\omega = 3$. (Here $m = 1$ and by necessity $\beta = \rho\omega/(\rho + \omega) = 2$, corresponding to $q = \sqrt{2m\beta} = 2$.) The constants of integration have been chosen so that $r(0) = \rho$.

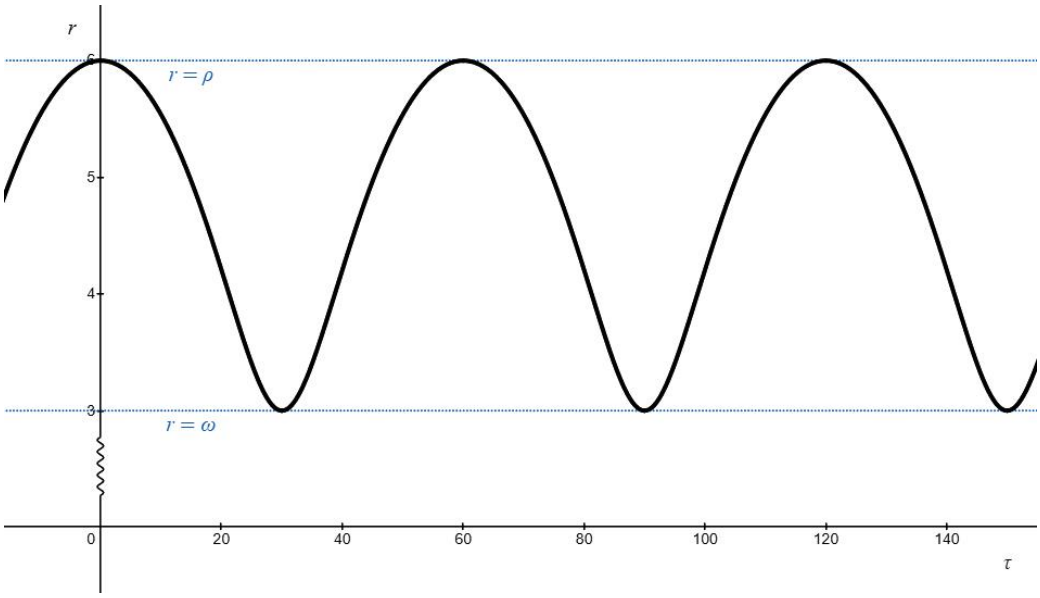

Figure 5 Periodic orbit $r(\tau)$ *between* $r = 3$ *and* $6\ (\beta = 2)$. *The period is* $27\pi/\sqrt{2} \approx 60$.

The period T of the orbit is

$$T = 2[\tau(\omega) - \tau(\rho)] = \frac{\pi}{\sqrt{2m}}(\rho + \omega)^{3/2}\,.$$

D. Geodesics in Penrose spacetime diagrams

Radial geodesics appear in Penrose diagrams as worldlines connecting i^- (past timelike infinity) and i^+ (future timelike infinity).[11] Figure 6 illustrates unbound and bound geodesics.[12] The unbound orbit (left) reaches a minimum radius $\beta = 2$. The bound orbit (right) oscillates between $\rho = 3$ and $\omega = 2$, so here $\beta = \rho\omega/(\rho + \omega) = 1.2$, corresponding to $q = \sqrt{2m\beta} \approx 1.549$. The oscillations have been exaggerated in this illustration: in an accurate diagram the bound geodesic would lie imperceptibly close to the worldline $r = 3$, since it oscillates with period $T \approx 25$. Only intense magnification around i^- or i^+ would reveal the oscillation. Penrose diagrams can be misleading since they compress infinite volumes of spacetime into the corners.

[11] A Penrose (or conformal) diagram is a spacetime diagram using maximally-extended coordinates (e.g., Kruskal-Szekeres coordinates for a Schwarzschild black hole) where the metric has been conformally rescaled to include the points at infinity. See Misner, Thorne and Wheeler [6] (§34.2) for a general discussion of Penrose diagrams, and Hawking and Ellis [4] or D'Inverno [9] for a detailed discussion of Penrose diagrams for Reissner-Nordström black holes.

[12] In both examples we choose $m = 1$. Different values of β are assumed for illustrative purposes.

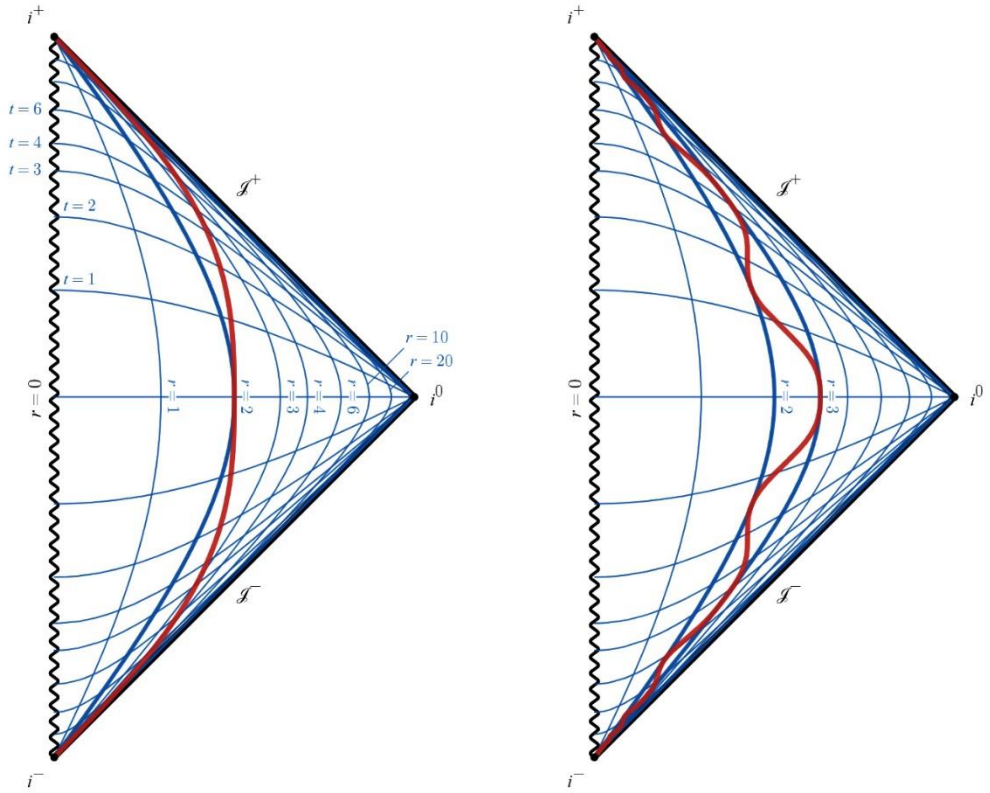

Figure 6 Penrose diagram for the superextremal case. Left: unbound orbit $(\beta = 2)$. *Right: bound orbit between* $\rho = 3$ *and* $= 2$ $(\beta = 1.2)$.

C. Geodesics starting from $r = \rho < \beta$

Equation of motion. Consider an object which starts from rest at radius $\rho < \beta$. We analyze the motion as above. From (9):

$$e^2 = 1 + \frac{2m(\beta - \rho)}{\rho^2}. \tag{27}$$

Thus, the potential energy increases without bound as $\rho \to 0$, so the singularity is infinitely repulsive. The equation of motion is given by (22):

$$\dot{r}^2 = \left(-\frac{2m}{\rho + \omega}\right)\frac{(r-\rho)(r-\omega)}{r^2} \tag{28}$$

where it is remembered that $\rho < \beta$ implies $\omega < 0$ and $\rho + \omega < 0$, so that $\dot{r}^2 > 0$ for $r > \rho$.

To confirm the direction of motion, we use (24) to find $\ddot{r}(\rho) = m(2\beta - \rho)/\rho^3 > 0$. Since ρ is the only point where $\dot{r}$ vanishes, the direction of motion is always outgoing. Accordingly, we take the positive square root in (28) and obtain

$$\dot{r} = \sqrt{\frac{2m}{|\rho+\omega|}}\frac{\sqrt{(r-\rho)(r-\omega)}}{r}\,. \tag{29}$$

We will see below that the orbit is unbounded (as in the case $\rho = \beta$).

Shell speeds. It is convenient to return to (20) for the equation of motion, expressed in terms of β and ρ:

$$\dot{r}^2 = \frac{2m(r-\beta)}{r^2} - \frac{2m(\rho-\beta)}{\rho^2}$$

which we re-write (since $\rho < \beta$):

$$\dot{r} = \sqrt{\frac{2m(\beta-\rho)}{\rho^2} - \frac{2m(\beta-r)}{r^2}}\,. \tag{30}$$

The object accelerates outward from ρ and passes shell observer $\mathcal{S}_\beta$ with radial speed $\dot{r}(\beta) = \sqrt{2m(\beta-\rho)}/\rho$, which $\to\infty$ as $\rho\to 0$. However, $\mathcal{S}_\beta$ sees the object pass by with speed

$$v_\beta = \frac{\dot{r}(\beta)}{e} = \frac{\sqrt{2m(\beta-\rho)}}{\sqrt{\rho^2+2m(\beta-\rho)}} < 1\,.$$

Therefore, as $\rho\to 0$ we find that $\dot{r}(\beta)\to\infty$ but $v_\beta \to 1$! This disparity is not caused by curvature at $r=\beta$; in fact, spacetime here is actually flat. It is because $e\longrightarrow\infty$ as $\rho\to 0$. As $\rho\to 0$ the object's acceleration and speed increase, and time dilation separates $d\tau_r$ and $d\tau_g$.

Generalizing the last observation: as $\rho\to 0$ we find by (30) that $\dot{r}\to\infty$ everywhere in the interval $\rho < r \le \beta$. However, a shell observer $\mathcal{S}_r$ in this interval sees the object traveling with speed

$$v_r = \frac{\dot{r}}{e} = \frac{\sqrt{\frac{2m(\beta-\rho)}{\rho^2} - \frac{2m(\beta-r)}{r^2}}}{\sqrt{1+\frac{2m(\beta-\rho)}{\rho^2}}} = \frac{\sqrt{2m(\beta-\rho) - \frac{2m\rho^2(\beta-r)}{r^2}}}{\sqrt{\rho^2+2m(\beta-\rho)}}\,. \tag{31}$$

Figure 7 shows v_r for various values of ρ. Note when $\rho=\beta$, (31) gives $v_r = \sqrt{2m(r-\beta)}/r$, which agrees with (17).

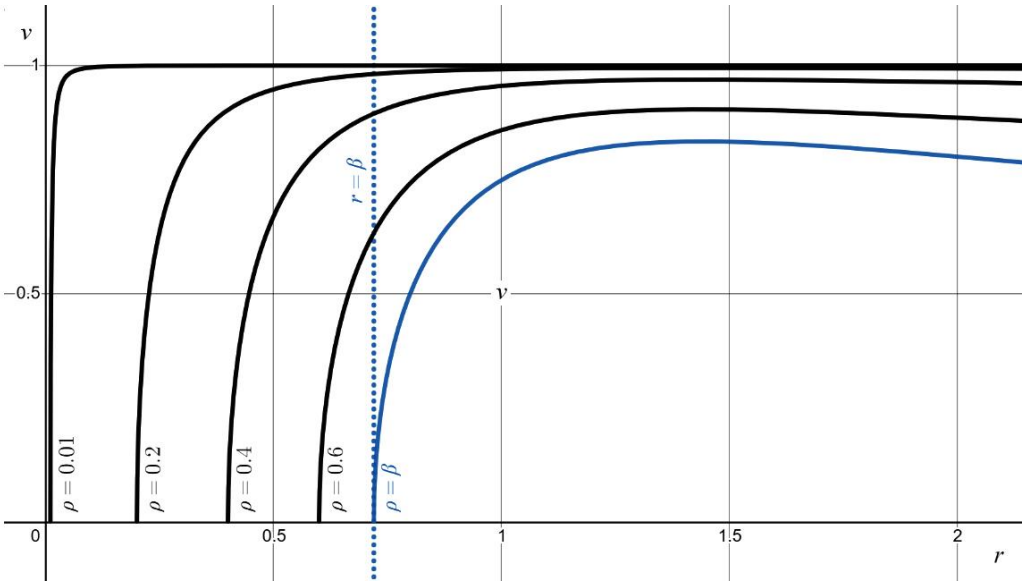

Figure 7 Shell speed v_r for geodesics starting at rest from $\rho = 0.01, 0.2, 0.4, 0.6$. Blue curve is the geodesic starting from rest at $= \beta = 0.72$ $(q = 1.2)$.

Remarks:

(i) $\lim_{\rho \to 0} v_r = 1$ for all r (a consequence of $e \to \infty$).

(ii) v_r attains a maximum at $r = 2\beta$.

(iii) For $\rho < \beta$ and $r \gg 0$:

$$v_r \approx \sqrt{\frac{2m(\beta - \rho)}{\rho^2 + 2m(\beta - \rho)}} = \left(1 + \frac{\rho^2}{2m(\beta - \rho)}\right)^{-1/2} = \frac{1}{\sqrt{1 + 2m|\rho + \omega|}}.$$

Thus, geodesics that start from $\rho < \beta$ behave differently at large r than geodesics that start at $\rho = \beta$. When $\rho < \beta, v_r$ trends down to a constant as $r \to \infty$; while for $\rho = \beta, v_r$ falls off like $1/\sqrt{r}$ (see the second equation in (19)). This is not apparent in Figure 7 but becomes clearer if the plot is rescaled with the r-axis logarithmic (Figure 8). The reason for this is clear. From (9) an object starting from rest at β has $e = 1$, which is also the energy of an object that falls from rest at infinity. But when $\rho < \beta$, (27) shows that $e > 1$. Hence, the situation is analogous to a projectile leaving the Earth with a speed exceeding the escape velocity: if $\rho < \beta$ the object travels to infinity with excess kinetic energy $e = 1$.

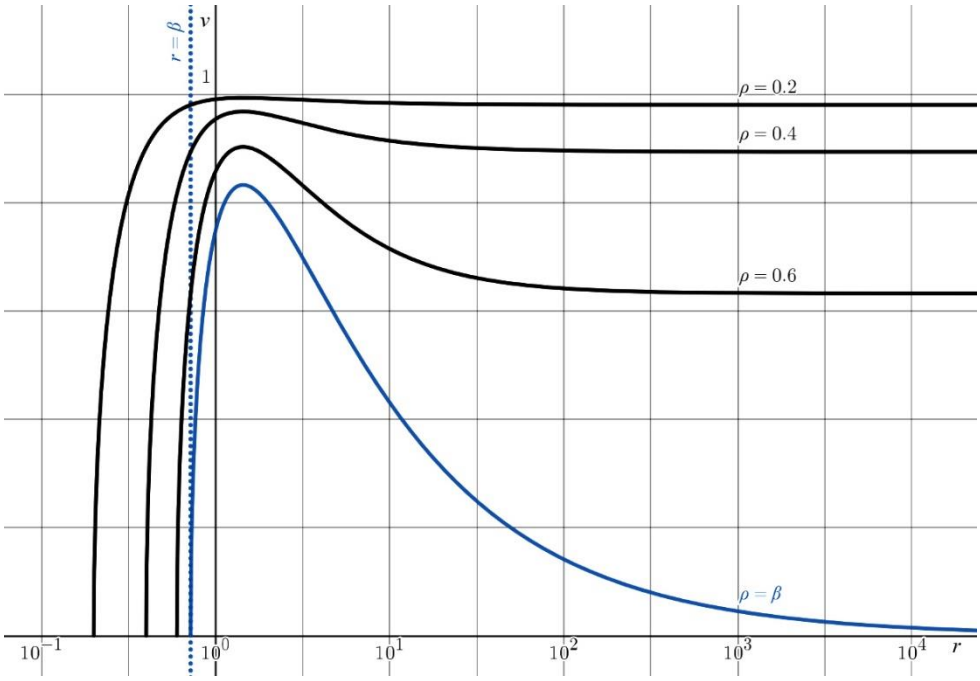

Figure 8 The same plot as in Figure 7 except the r-axis is logarithmic. When $\rho = \beta$ the trajectory is the reverse of an object in free fall from rest at infinity $(e = 1)$. When $\rho < \beta$, $e > 1$ and the object travels to infinity with a surplus of kinetic energy.

Geodesic trajectories. Outbound trajectories can be determined by integrating (29):

$$\tau = \int \frac{dr}{\dot{r}} = \sqrt{\frac{|\rho + \omega|}{2m}} \int \frac{r dr}{\sqrt{(r-\rho)(r-\omega)}} \tag{32}$$

which yields

$$\tau = \sqrt{\frac{|\rho + \omega|}{2m}} \left\{ \sqrt{(r-\rho)(r-\omega)} - \frac{|\rho + \omega|}{2} \ln\left(2\sqrt{(r-\rho)(r-\omega)} + 2r + |\rho + \omega| \right) \right\} + C\,. \tag{33}$$

Figure 9 shows the trajectory $r(\tau)$ for various values of ρ. The constants C have been chosen so that $r(0) = \rho$ for each curve. The approximately linear behavior of $r(\tau)$ for $r \gg \beta$ is apparent in the curves with $\rho < \beta$. The curve in blue is the outgoing geodesic starting from rest at $\rho = \beta$, given by (18). For $\rho = \beta$, the curve $r(\tau)$ grows like $\tau^{2/3}$ when $r \gg \beta$ (see (19)), which is not apparent in the Figure 9 since the inflection point occurs at $r = 2\beta$. The shape of the curve would be revealed if the axes were rescaled.

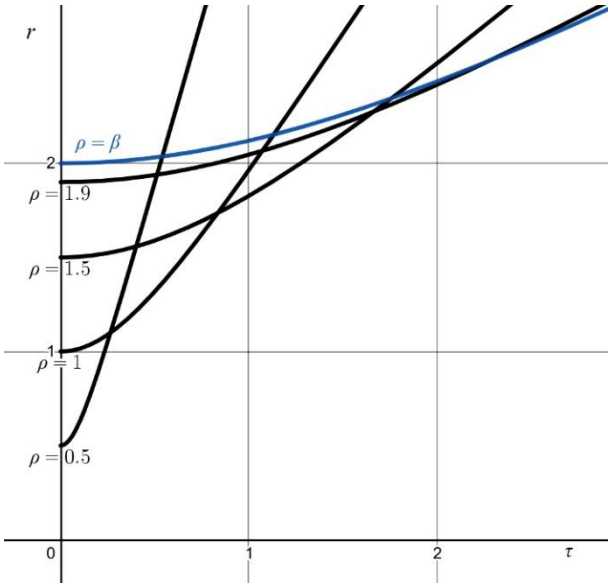

Figure 9 Trajectories $r(\tau)$ *of a geodesic starting from rest at* $r = \rho$ *for* $\rho = 0.5, 1, 1.5, 1.9$ $(\beta = 2)$. *Blue curve is the geodesic starting at rest from* $\rho = \beta$, *and grows* $\propto \tau^{2/3}$ *for* $r \gg \beta$.

F. River speed

"River speed" is a concept intended to convey the "speed of space" and provide an intuitive basis for geodesics in curved spacetime ([10]). Recall that for a Schwarzschild black hole, the metric is given by (1) with $f(r) = 1 - 2m/r$ and the equation of motion for a radial geodesic is $\dot{r}^2 = e^2 - (1 - 2m/r)$. An object that falls freely from rest at infinity $(e = 1)$ satisfies $\dot{r} = v_r = -\sqrt{2m/r}$. The speed $|v_r| = 0$ at $r = \infty$ and increases to $|v_r| = 1$ (light speed) at $r = 2m$. After crossing the event horizon $r = 2m$, the speed $|v_r| \to \infty$ as $r \to 0$. We think of a freely falling object as being carried along this geodesic as if floating on a river with current speed $v_r = -\sqrt{2m/r}$, referred to as the "river speed" (or "waterfall speed").

For a Schwarzschild black hole, shell observers cannot exist at $r \leq 2m$ where $|v_r| \geq 1$. In fact, the following are equivalent:

(i) $f(r) < 0$.

(ii) $|v_r| > 1$.

(iii) The unit vector $\hat{\mathbf{r}}$ points in a timelike direction. (34)

Proof: (i) ⇔ (ii): Follows from (4). (i) ⇔ (iii): From the metric (1), if $f(r) < 0$, then along the worldline $t =$ constant $(dt = 0)$ we have $ds^2 = dr^2/f(r)$. Hence $f(r) < 0 \Leftrightarrow ds^2 < 0$. (Similarly, along the worldline $\mathbf{x} =$ constant $(d\mathbf{x} = 0)$ we have $ds^2 = -f(r)dr^2$, so $f(r) < 0 \Leftrightarrow ds^2 > 0$, which means the unit vector $\hat{\mathbf{t}}$ points in a spacelike direction.) Note that the inequalities in (i) and (ii) can be replaced with equality if in (iii) "timelike" is replaced with "lightlike".

An object in free fall (starting from rest at infinity) is seen by a shell observer $\mathcal{S}_r$ to be traveling with speed given by (11):

$$v_r = \frac{\dot{r}}{e} = -\frac{\sqrt{2m(r-\beta)}}{r} \tag{35}$$

which vanishes at $r = \beta$ and is not defined (or imaginary) for $r < \beta$. Figure 1 illustrates v_r for Schwarzschild and Reissner-Nordström black holes.

We ask two questions:

(1) For $r \geq \beta$, can v_r defined by (35) be sensibly interpreted as river speed?

(2) Can we define river speed in the region $0 \leq r < \beta$?

The foregoing analysis enables us to respond as follows:

Question (1): An object starting from rest at $r = 2\beta$ does not move, since $\ddot{r} = 0 \Longrightarrow \dot{r} = 0$. Hence the river speed at 2β should be zero, whereas (35) gives $v_{2\beta} = -\sqrt{m/2\beta} = -m/q$, which is where $|v_r|$ attains its maximum value! Similarly, an object starting from rest at $r = \beta$ is accelerated outward, hence the river speed at β should be positive, but we have $v_\beta = 0$. Therefore, the answer is no: v_r fails to provide a sensible representation of river speed for radii smaller than $\approx 2\beta$.

Question (2): Geodesics that start from $\rho \leq \beta$ travel outward to infinity. Therefore, intuitively, space should be accelerating outward. From (31) a shell observer $\mathcal{S}_r$ in the region $0 < r \leq \beta$ sees $v_r \to 1$ as $\rho \to 0$ (see Figure 7). This is a consequence of the infinite repulsion of the singularity: as the initial position $\rho \to 0$ we require $e \to \infty$, propelling the object outward at a speed $v_r \to 1$. Note that shell observers are admissible everywhere since $f(r) > 0$.

Which starting point ρ shall we choose to define the geodesic that corresponds to river speed? Intuitively, we seek a geodesic that starts from rest $(\dot{r} = 0)$ at a point of unstable equilibrium where the acceleration is zero $(\ddot{r} = 0)$, such as $r = \infty$. But there are no such places with $r \leq \beta$. The radial velocity $\dot{r} = 0$ only at β, and $\ddot{r} = 0$ only at 2β. One may be tempted to try the geodesic starting from $\rho = 0$, but this geodesic has $v_r = 1$ for all r, which is not what we want. Hence, there is no sensible or consistent way to define river speed for $r < \beta$. The river model breaks down when $f(r)$ has local extrema.

Subextremal and Extremal Black Holes

The superextremal case is convenient for developing the essential features of geodesics without the additional complications present in the subextremal and extremal cases. However, superextremal singularities are probably unphysical for several reasons. First, the amount of charge

q equivalent to a stellar mass is enormous, and such a highly charged mass would quickly become neutralized by attracting opposite charge from its environment.[13] Second, the *weak cosmic censorship conjecture* asserts that nature does not permit "visible" or "naked" singularities. A "visible" singularity means that there exists a lightlike path from the singularity to $\mathscr{I}^+$ (future null infinity) that does not cross an event horizon.[14]

Our analysis and results in the superextremal case carry over to the subextremal and extremal cases since the equations of motion (5) are based on proper (geodesic) time. However, there will be changes in the measurements made by shell observers $\mathcal{S}_r$ and the far-away observer who measures all dynamical variables using r-t coordinates.

A. Location of geodesic turning points

In the region $r_- \le r \le r_+$, we have $r^2 f(r) = r^2 - 2mr + q^2 \le 0$ and therefore $|v_r| \ge 1$ by (4). This region is a black hole where no shell observers can exist.

The following fact is useful. Algebra (or Figure 10) shows that $|q| > 0$ implies:

$$\begin{aligned} &\beta < r_- < 2\beta < r_+ \quad \text{(subextremal case)} \\ &\beta < r_\pm = 2\beta = m \quad \text{(extremal case)} \end{aligned} \tag{36}$$

Hence, $r = \beta$ lies strictly ***within the inner horizon***. This is not surprising since $\dot{r}(\beta) = 0$, which cannot occur inside the black hole. Furthermore, $r = 2\beta$ lies ***between the horizons***. By (24), $\ddot{r}(2\beta) = 0$, so that an object placed at rest at $r = 2\beta$ remains at rest. While this would be true in the superextremal case, it cannot be true in the subextremal case since $r = 2\beta$ lies inside a black hole. There is no paradox; the initial condition $\dot{r}(2\beta) = 0$ is not a valid assumption.

We may obtain some perspective on the black hole by considering its dimensions for various values of $0 < |q| \le m$, as shown in Figure 10 (where we take $m = 1$). Except when the black hole is nearly extremal, the inner horizon lies very close to β, so an ingoing object in free fall decelerates rapidly between 2β and β. For small $|q|$, the black hole region $r_- \le r \le r_+$ occupies nearly the entire interval $[0, 2m]$. The interior region $0 \le r < r_-$ is consequently very narrow.[15]

---

[13] An electric charge q equivalent to the mass of the sun $GM_\odot/c^2 = 1{,}477\ \mathrm{m}$ has charge $q = 1{,}477 \div 8.62 \times 10^{-18}\ \mathrm{m/C} = 1.71 \times 10^{20}\ \mathrm{C} = 1.07 \times 10^{39}$ elementary charges. This is approximately the number of electrons (or protons) in 4 trillion kg of iron, equal to a cube of iron 798 meters wide.

[14] See Penrose [11] and Wald [12].

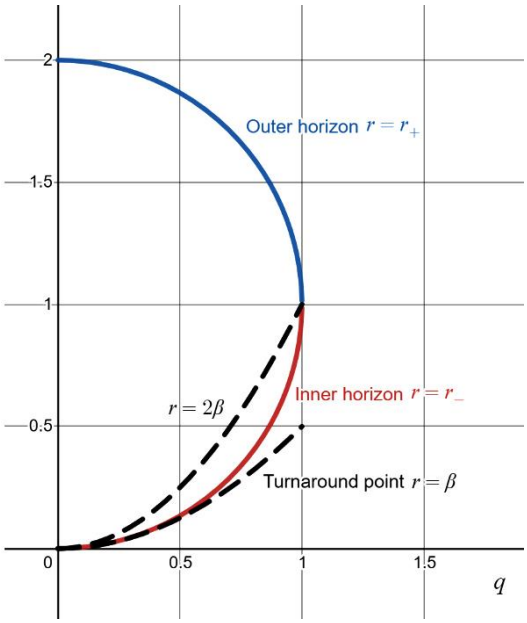

Figure 10 Variation (with q) of the radius of the outer horizon $r = r_+$, inner horizon $r = r_-$, turnaround point $r = \beta$, and "zero acceleration" point $r = 2\beta$.

Figure 11 shows the relationship between the turning points ρ and $\omega = \rho\beta/(\rho - \beta)$. Note that for geodesic motion starting from rest at $r = \rho$ *outside* the black hole:

(i) If $\rho > r_+$, then $\omega < r_-$.

(ii) If $\beta < \rho < r_-$, then $\omega > r_+$.

Thus, the turning points of the geodesic always lie outside the black hole, as they must. When $\rho \leq \beta$ we have $\omega < 0$, which signals that there is no opposite turning point — the trajectory is unbounded (r increases to infinity).

---

[15] For small q/m, the inner horizon $r_- = m\left[1 - \sqrt{1 - (q/m)^2}\right] \approx q^2/2m$. For a $10M_\odot$ black hole $(m = 14.77\ \text{km})$ with $q/m = 10^{-12}$ $(\Longrightarrow q = 1.7 \times 10^9\ \text{C})$ we find that $r_- = 7.4 \times 10^{-21}\ \text{m}$. This is so close to the singularity that any object would be destroyed by tidal forces (or extreme deceleration).

Conversely, the charge required for $r_- = \ell_P$ (the Planck length) is $q \approx \sqrt{2m\ell_P}$. For a $10M_\odot$ black hole this is $q \approx \sqrt{2(14{,}770)(1.6 \times 10^{-35})} = 6.87 \times 10^{-16}\ \text{m} \approx 80\ \text{C}$. A star formed from neutral gas may have a positive charge up to $\approx 100\ \text{C}$ per solar mass (see [13]), so the inner event horizon of a charged black hole is unlikely to be significantly larger than a few multiples of the Planck length.

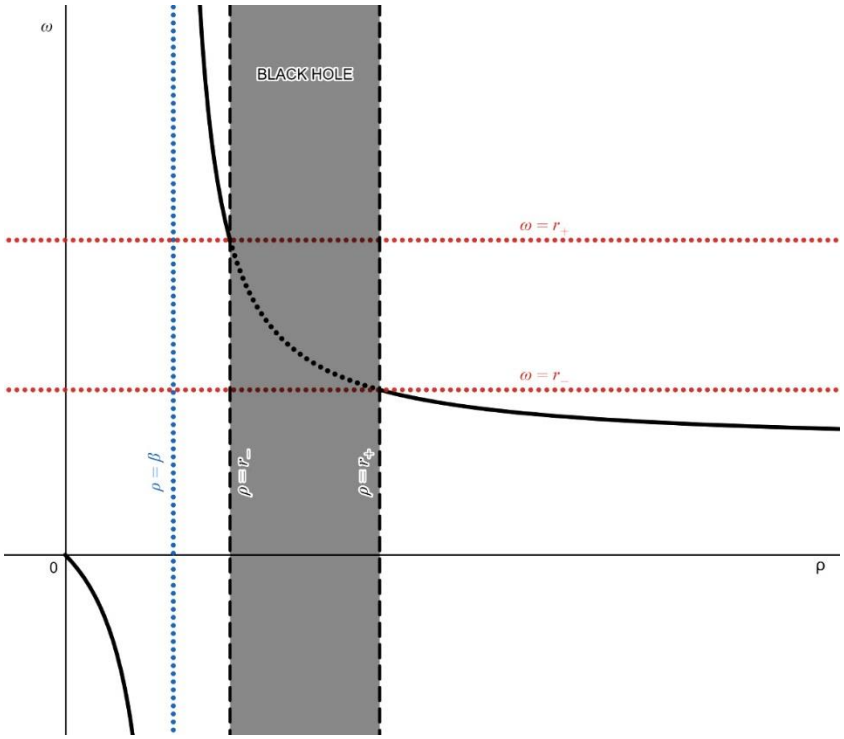

Figure 11 Relationship between ρ *and* $\omega(\rho) = \rho\beta/(\rho - \beta)$. *The turning points* ω *and* ρ *lie outside the black hole when* $\rho > r_+$ *or* $\rho < r_-$. *When* $\rho \leq \beta$ *the trajectory is unbounded.*

B. River speed (revisited)

The river-speed model was partly motivated to provide an intuitive explanation why motion inside a Schwarzschild black hole is always toward the singularity (namely $v_r < -1$ means that the inward "flow of space" is faster than the speed of light). In the superextremal case there is no black hole, while in the subextremal case there is a black hole in the spherical annulus $r_- \leq r \leq r_+$. (In the extremal case there is a single horizon at $r = m$, but the region $r \leq m$ appears as a "black hole" to an outside observer.)

Does the river model stand up any better in the subextremal or extremal cases? No: the model fails in the Reissner-Nordström metric due to the effective potential having both repulsive and attractive characteristics, which is reflected in the local extremum of $f(r)$, not the number of zeros of $f(r)$.[16] Since the geodesic trajectories parameterized by proper time are the same in all cases (superextremal, extremal, subextremal), the arguments of the previous section concerning "river speed" remain valid, with one minor exception discussed below.

[16] Recall from (7) that $v_r = 1 - f(r)$, so we can infer from Figure 1 that $f(r)$ has a single extremum. Alternatively, from (8) we can compute directly: $f'(r) = 2m(r - \beta)/r^3$, which implies that $f(r)$ has a local maximum at $r = \beta$.

Since $|v_r| \geq 1$ inside the black hole region $r_- \leq r \leq r_+$, the river model provides the same intuitive explanation why motion is toward the singularity as with the Schwarzschild metric. But the model breaks down for the same reasons as given in the superextremal case. Eqn. (36) shows that $r = 2\beta$ (where $\ddot{r}$ changes sign) is located inside the black hole. Therefore, the previous demonstration that the model fails at $r = 2\beta$ must be modified slightly, since it is impossible for an object to start from rest inside the black hole. Instead, we imagine releasing an object at $r = 2\beta$ with a small (inward) velocity. The object would initially accelerate very slowly because $\ddot{r}(\beta) = 0$. However, we still have $v_{2\beta} = -m/q$, which approaches $-\infty$ as $q \to 0$. Thus, we conclude again that v_r cannot be interpreted as the "speed of space."

C. Free fall times

The dynamics of an object in free fall from infinity are the same as in the superextremal case. Eqn. (10) gives the equation of motion $\dot{r} = \pm\sqrt{2m(r-\beta)}/r$, so the object falls through both event horizons and turns around at $r = \beta$. Trajectories are given by (14) and (18) and appear as in Figure 2. Behavior at the turnaround point becomes more cusp-like as $\to 0$ $(\beta \to 0)$.

The proper time to fall from any finite $r = R$ to $r = \beta$ is given by (15). Hence, an object in free fall crosses both event horizon(s) in finite proper time. In the extremal and subextremal cases, the role of the outer horizon is like the event horizon of a Schwarzschild black hole. In particular, the far-away observer who measures all dynamical variables in r-t coordinates never sees a free-falling object reach $r = r_+$. The verification is straightforward. Write

$$f(r) = 1 - \frac{2m}{r} + \frac{q^2}{r^2} = \frac{(r-r_+)(r-r_-)}{r^2}. \tag{37}$$

From the t-equation of motion (5), $dt/d\tau_g = 1/f(r)$. Hence the far-away observer measures the time to fall from $r = R$ to $r = r_+$:

$$\Delta t = \int_{r=R}^{r=r_+} dt = \int_R^{r_+} \frac{d\tau_g}{f(r)} = \int_R^{r_+} \frac{dr}{\dot{r} f(r)} = \int_R^{r_+} \frac{-r}{\sqrt{2m(r-\beta)}} \cdot \frac{r^2 dr}{(r-r_-)(r-r_+)}$$

$$= \int_{r_+}^{R} \frac{r^3 dr}{\sqrt{2m(r-\beta)}(r-r_-)(r-r_+)} = \infty \tag{38}$$

since the integrand behaves like $\text{constant}/(r-r_+)$ in a neighborhood of r_+.

This also implies that a shell observer $\mathcal{S}_\rho$ never sees an object reach $r = r_+$. From (3) we have $\tau_\rho = \sqrt{f(\rho)}\, dt$. Hence $\mathcal{S}_\rho$ measures the time to fall from $r = R$ to $r = r_+$:

$$\Delta\tau_\rho = \int_{r=R}^{r=r_+} d\tau_\rho = \int_R^{r_+} \frac{d\tau_\rho}{dt} dt = \sqrt{f(\rho)} \int_R^{r_+} \frac{dr}{\dot{r} f(r)} = \infty$$

by the same calculation as in (38).

D. A paradox

The previous result presents a paradox. $\mathcal{S}_r$ sees an ingoing object in free fall toward the black hole approaching — but never reaching — the outer horizon r_+. However, in finite proper time the object crosses both horizons, turns around at $r = \beta$, crosses both horizons again, and travels outward along the same radial line — to collide with itself outside of r_+ in full view of $\mathcal{S}_r$! The explanation is provided by the maximally-extended geometry for a subextremal Reissner-Nordström black hole.

E. Penrose diagram for subextremal black hole

Figure 12 illustrates the Penrose diagram for the subextremal case. (Hawking and Ellis [4] and D'Inverno [9] discuss Penrose diagrams for all three cases of Reissner-Nordström black holes: superextremal, extremal and subextremal.[17]) The trajectory in purple shows the bound orbit of an object in free fall starting from rest at $\rho > r_+$. The trajectory can be described as follows:

1. The object starts from rest at $r = \rho$ in *Our Universe* and begins to accelerate inward.
2. At $r = r_+$ it enters the black hole, where it cannot be seen by outside observers.
3. At $r = 2\beta$ the object stops accelerating inward and begins to decelerate.
4. The object exits the black hole at $r = r_-$ and enters *Our Wormhole:* the region $0 \le r < r_-$.
5. At $r = \omega$ the object comes to a stop and begins moving outward.
6. Between $r_- \le r \le r_+$ it travels through a *white hole* (accelerating until $r = 2\beta$ and decelerating afterward).
7. At $r = r_+$ the object emerges into *Our New Universe*.

[17] For a Schwarzschild black hole, a spacetime diagram using maximally-extended (Kruskal-Szekeres) coordinates reveals a parallel space or universe, which also has an event horizon bordering the black hole. Only a spacelike trajectory can traverse the black hole from one universe to the other, so no object (including a photon) can travel between the two universes. In the Reissner-Nordström case, the black hole occupies the region $r_- \le r \le r_+$. Interior to the black hole $(r < r_-)$ is a *wormhole* in which the singularity $r = 0$ lies. The singularity is timelike (unlike the Schwarzschild singularity, which is spacelike) and therefore need not lie on the timelike worldline of an object passing through the wormhole.

To outside observers in *Our Universe*, the object approaches r_+ asymptotically as $t \to \infty$. To outside observers in *Our New Universe*, the object has been emerging from r_+ since $t = -\infty$.

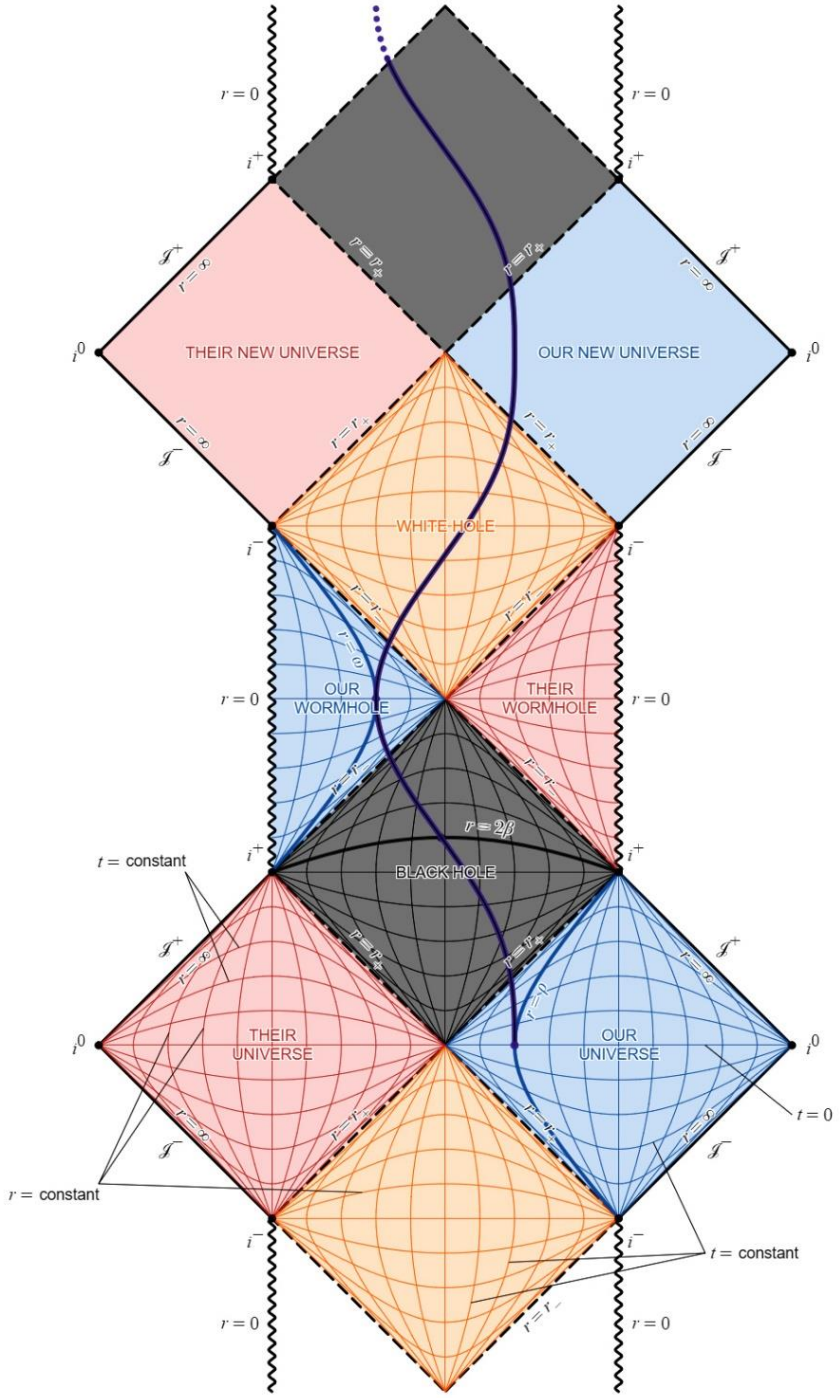

Figure 12 Penrose diagram for a subextremal Reissner-Nordström black hole. The purple trajectory is a bound geodesic starting at $r = \rho$ in Our Universe. An unbound orbit would start at i^- in Our Universe and finish at i^+ in Our New Universe.

Finding the right wormhole. Figure 12 shows the geodesic passing through *Our Wormhole* and into *Our New Universe*. However, timelike trajectories into *Their Wormhole* and *Their New Universe* are also possible. To see why the geodesic must follow the trajectory shown in Figure 12, note the directions in which the t-coordinate increases and decreases in the various regions, shown in Figure 13.

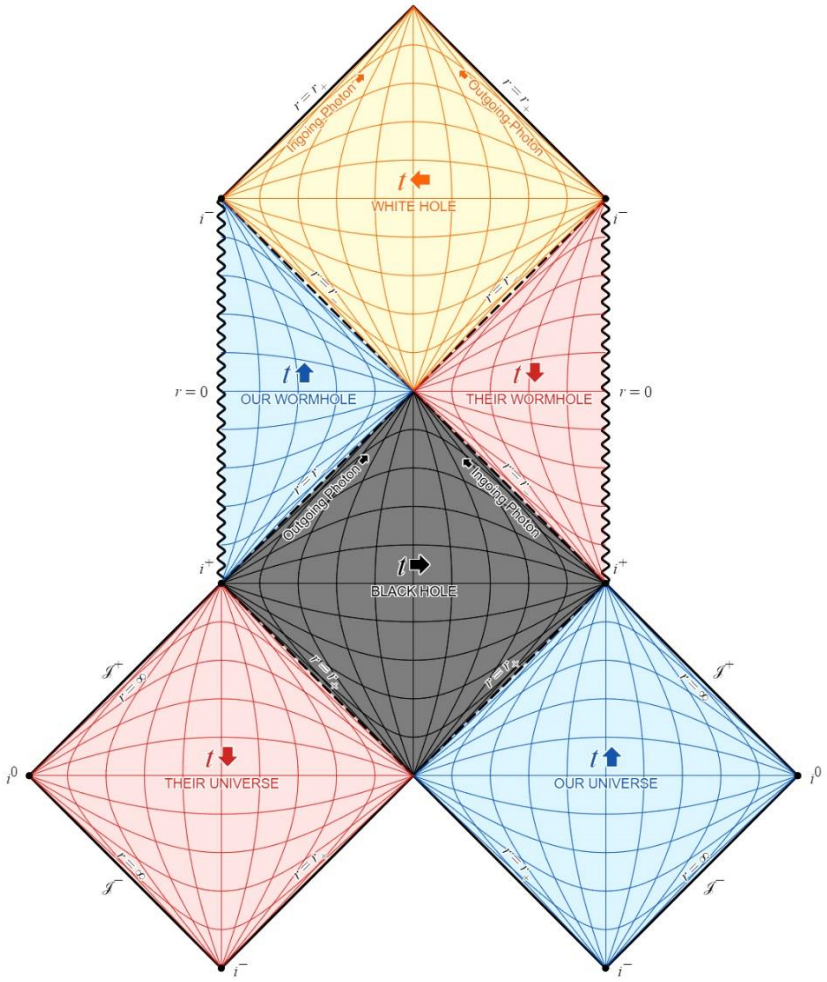

Figure 13 *Penrose diagram showing directions of increasing* t*-coordinate.*

If an ingoing trajectory, originating in *Our Universe* and passing through the black hole, were to enter *Their Wormhole*, then somewhere inside the black hole dt must change from negative to positive (the worldline has a vertical tangent). Therefore, $dt = 0$ somewhere along the trajectory. However, the t-equation of motion (5) says $dt = [e/f(r)]d\tau$, so $dt < 0$ everywhere inside the black hole; in particular, $dt \neq 0$. Therefore, ***the geodesic must enter Our Wormhole.*** A similar argument applies inside the white hole to guarantee that the geodesic enters *Our New Universe*.

Using thrusters to influence the trajectory, a spaceship inside the black hole can traverse the t-coordinate forwards (right) or backwards (left) and enter either *Our Wormhole* or *Their Wormhole*. Likewise, inside the white hole a spaceship can steer a course into either *Our New Universe* or *Their New Universe*. Figure 14 illustrates several such trajectories.

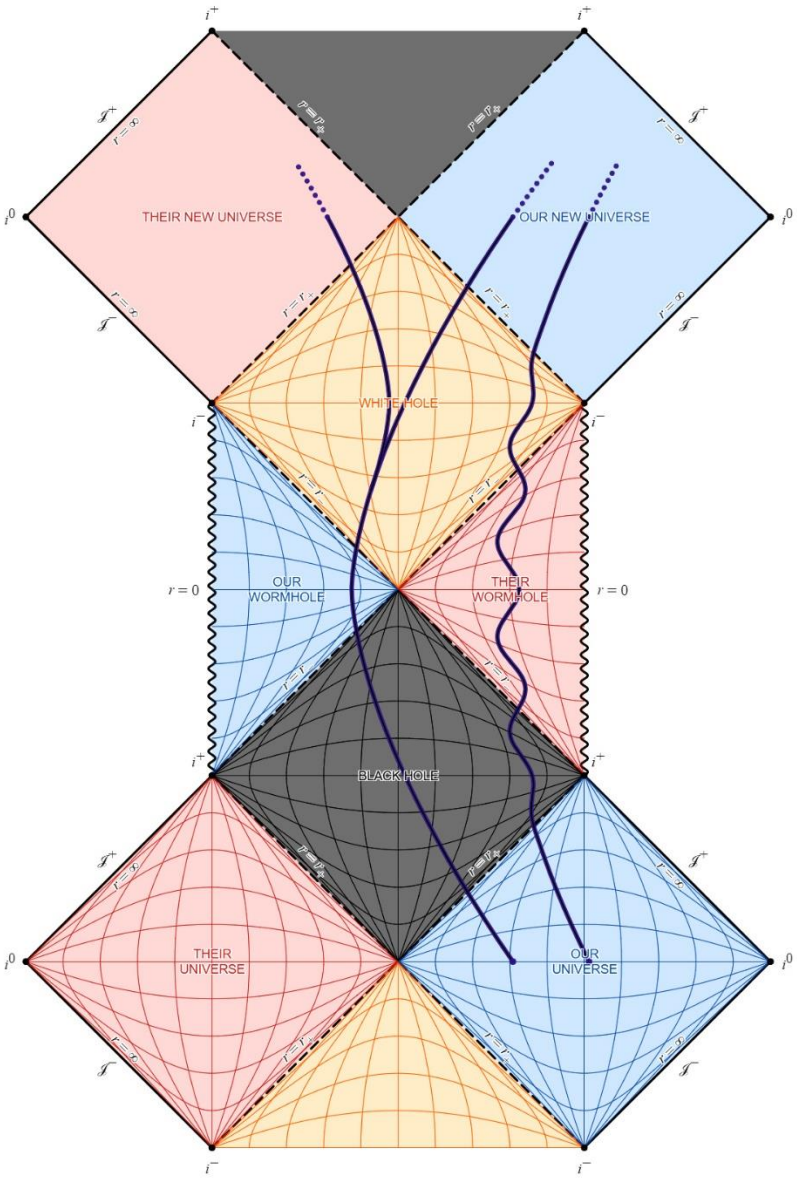

Figure 14 *Penrose diagram showing various non-geodesic trajectories.*

As an aside, it is possible to navigate within the black and white holes and wormholes using geodesics. A spaceship captain lost in one of these regions can follow photons coming from *Our Universe*. The worldline of an ingoing photon from *Our Universe* passes through the black hole at a 135°-angle in the Penrose diagram, enters *Our Wormhole*, and "reflects" off the singularity $r = 0$.

(The photon actually passes through the singularity and changes from an ingoing photon to an outgoing photon.) The photon continues at a 45°-angle through the white hole and enters *Our New Universe*. Hence, a spaceship can locate *Our New Universe* by stationing a source of recognizable photons at his point of departure (for instance, an antenna sending radio waves transmitting Beethoven's Fifth Symphony), and then follow these photons into *Our New Universe*.[18]

F. Extremal black holes

Infinite distance to the horizon. In the subextremal case, a shell observer $\mathcal{S}_r$ outside the black hole uses (1) to measure the proper length between two shells of radius r and $r+dr$:

$$d\lambda = \frac{|dr|}{\sqrt{f(r)}} = \frac{r|dr|}{\sqrt{(r-r_+)(r-r_-)}}.$$

Therefore, $\mathcal{S}_r$ measures the distance from $r=R$ to the outer horizon r_+:

$$\Delta\lambda = \int_{r_+}^{R} \frac{dr}{\sqrt{f(r)}} = \int_{r_+}^{R} \frac{rdr}{\sqrt{(r-r_+)(r-r_-)}} < \infty\,.$$

$\mathcal{S}_r$ measures a finite distance to the outer horizon, even though he never sees a falling object reach it. (In the superextremal case, we also have $\Delta\lambda<\infty$, since $f(r)>0$ everywhere.)

In the extremal case, however, $r_+ = r_- = m$ where $1/f(r)$ has a double pole. Therefore

$$\Delta\lambda = \int_{m}^{R} \frac{dr}{\sqrt{f(r)}} = \int_{m}^{R} \frac{rdr}{r-m} = \infty\,.$$

Thus, the horizon is *invisible*, being infinitely far away.

Behind the horizon. In the extremal case there is a single horizon $r_\pm = m$ bounded by regions where $f(r)>0$. Hence, there are no black or white holes where $\hat{\mathbf{r}}$ points in a timelike direction (see [4] or [9] for the relevant Penrose diagram). In *Our Universe* this is a "future horizon", since ingoing objects are observed to reach the horizon at $t=\infty$, just as with subextremal and Schwarzschild black holes.

[18] This is somewhat fanciful. The inner horizon is considered unstable in the presence of any mass or energy. An infinite blueshift at the inner horizon was first pointed out by Penrose [14] who suggested this would destabilize the geometrical structure. This instability was analyzed by Poisson and Israel [15] who termed it "mass inflation"; see also [16]. We are assuming the black hole is "empty", meaning empty of charge, matter, or radiation (but not of a static electric field) except at the singularity.

An ingoing object crosses the horizon and enters a wormhole, in which all timelike paths lead to a *New Universe*. It departs the wormhole through another horizon — a "past horizon" in the *New Universe*, in which the object appears to have been emerging since $t = -\infty$ (as with white holes). The region $r \leq m$ in *Our Universe* is a "black hole" in the sense that nothing which falls into the region can ever get out, but not in the sense where $f(r) < 0$ and $\hat{\mathbf{r}}$ points in a timelike direction. The region $r \leq m$ is the connecting region (wormhole) between two universes: the black and white holes which are present in the subextremal case have been squeezed out of existence as the inner and outer horizons merge into one. Similarly, the region $r \leq m$ could be called a "white hole" in the *New Universe* in the sense that no timelike path from the *New Universe* can enter it.

Whether or not the wormhole should be termed a "black hole" in *Our Universe* and a "white hole" in the *New Universe* is somewhat academic, since ***the horizons are invisible*** to outside observers, as shown above. Therefore, their presence would be difficult to detect. Moreover, an extremal "black hole" would be unstable, since the addition of the smallest amount of charge would make it either superextremal or subextremal. (But then the situation would no longer be static.)

Conclusion

We have shown that the Reissner-Nordström metric

$$ds^2 = -\left(1 - \frac{2m}{r} + \frac{q^2}{r^2}\right)dt^2 + \frac{dr^2}{1 - 2m/r + q^2/r^2} + r^2 d\theta^2 + (r\sin\theta)^2 d\phi^2$$

gives rise to a variety of interesting behaviors with respect to timelike geodesics (the trajectories of uncharged particles with positive mass). Examining only radial geodesics, we found that the singularity has a gravitationally repulsive character. Geodesics starting from rest at infinity or at $r < 2\beta = q^2/m$ have unbound orbits which go to infinity, while geodesics starting from rest at r between 2β and ∞ result in bound orbits. This behavior holds in all cases (superextremal, extremal and subextremal) with the proviso that in the subextremal/extremal cases the turnaround points of bound orbits lie outside the black hole region $r_- \leq r \leq r_+$.

Because of the behavior (extrema) of the coefficients of dt^2 and dr^2 in the metric, we find that the commonly cited "river model" to explain motion within black holes fails in the Reissner-Nordström case. It is immediately obvious that a problem with the river model must arise, since the shell-observer speed $v_r = -\sqrt{2m/r}$ in the Schwarzschild metric is replaced by $v_r = -\sqrt{2m/r - q^2/r^2}$, which is imaginary for $r < q^2/2m$. By analyzing geodesics at $r = \beta$ (where $\dot{r} = 0$ for a geodesic starting from rest at infinity) and 2β (where $\ddot{r} = 0$) we deduce that v_r cannot be interpreted as the "speed of space."

We have not extended the analysis to lightlike geodesics. Unlike timelike geodesics, lightlike (radial) geodesics pass through the singularity. To see this in the superextremal case, set $ds^2 = 0$ in (1) to obtain $dr/dt = \pm f(r) = \pm(1 - 2m/r + q^2/r^2)$ and integrate:

$$t(r) = \pm\left\{r + m\ln(r^2 - 2mr + q^2) + \frac{2m^2 - q^2}{\sqrt{q^2 - m^2}}\arctan\left(\frac{r - m}{\sqrt{q^2 - m^2}}\right)\right\} + C\,.$$

Setting $r = 0$ yields a well-defined value of t, and we can make $t(0) = 0$ by suitable choice of C. See [17] and [18] for further details. We have also omitted the treatment of non-radial geodesics [19,20] and the motion of charged particles [21,22] in Reissner-Nordström geometry, as well as the quantum and thermodynamic characteristics of Reissner-Nordström black holes [23-25]. Details can be found in the references.

References

[1] K. Schwarzschild, "Über das gravitationsfeld eines massenpunktes nach der Einsteinschen theorie", Sitzungsberichte der Königlich Preussischen Akademie der Wissenschaften (Berlin), 189-196 (1916). Reprinted in English: "On the gravitational field of a mass point according to Einstein's theory", General Relativity and Gravitation, 35, 951-959 (2003).

[2] H. Reissner, "Über die Eigengravitation des elektrischen feldes nach der Einsteinschen theorie", Annalen der Physik, 50, 106–120 (1916).

[3] G. Nordström, "On the energy of the gravitational field in Einstein's theory", Proceedings of the Koninklijke Nederlandse Akademie van Wetenschappen, 20, 1238–1245 (1918).

[4] S. W. Hawking and G. F. R. Ellis, "The large scale structure of space-time", Cambridge: Cambridge University Press (1973).

[5] R. Wald, "General relativity", Chicago: Chicago University Press (1984).

[6] C. W. Misner, K. S. Thorne and J. A. Wheeler, "Gravitation", W. H. Freeman (1973).

[7] T. Padmanabhan, "Gravitation: Foundations and frontiers", Cambridge: Cambridge University Press (2010).

[8] T. Dray, "Differential forms and the geometry of general relativity", Boca Raton, Florida: CRC Press (2015).

[9] R. D'Inverno, "Introducing Einstein's relativity", Oxford: Oxford University Press (1992).

[10] A. J. S. Hamilton and J. P. Lisle, "The river model of black holes", American Journal of Physics, 76, 519-532 (2008).

[11] R. Penrose, "The question of cosmic censorship", Journal of Astrophysics and Astronomy, 20, 233–248 (1999).

[12] R. Wald, "Gravitational collapse and cosmic censorship", In B. Iyer and B. Bhawal (Eds.), "Black holes, gravitational radiation and the universe: Essays in honor of C. V. Vishveshwara", Springer Netherlands, 100, 69–85 (1999).

[13] S. Ray, A. L. Espíndola, M. Malheiro, J. P. S. Lemos and V. T. Zanchin, "Electrically charged compact stars and formation of charged black holes", Physical Review D, 68, 084004 (2003).
[14] R. Penrose, "Structure of space-time," In C. M. de Witt and J. A. Wheeler (Eds.), "Battelle rencontres: 1967 lectures in mathematics and physics", New York: W. A. Benjamin, Inc., 121–235 (1968).
[15] E. Poisson and W. Israel, "Internal structure of black holes", Physical Review D, 41, 1796-1809 (1990).
[16] A. J. S. Hamilton and P. Avelino, "The physics of the relativistic counter-streaming instability that drives mass inflation inside black holes", Physics Reports, 495, 1–32 (2010).
[17] G. Eskin, "Behavior of null geodesics in the interior of Reissner-Nordstrom black hole", Reviews in Mathematical Physics, 31, 1950021 (2019).
[18] N. Dadhich and P. P. Kale, "Timelike and null geodesics in the Nordström field", Pramana – Journal of Physics, 9, 71–77 (1977).
[19] P. Pradhan and P. Majumdar, "Circular orbits in extremal Reissner Nordstrom spacetimes", Physics Letters A, 375, 474-479 (2011).
[20] D. Pugliese, H. Quevedo and R. Ruffini, "Circular motion of neutral test particles in Reissner-Nordström spacetime", Physical Review D, 83, 024021 (2011).
[21] S. Grunau and V. Kagramanova, "Geodesics of electrically and magnetically charged test particles in the Reissner-Nordström space-time: Analytical solutions", Physical Review D, 83 (4), 044009 (2011).
[22] D. Pugliese, H. Quevedo and R. Ruffini, "Motion of charged test particles in Reissner–Nordström spacetime", Physical Review D, 83, 104052 (2011).
[23] J. Mäkelä and P. Repo, "A quantum mechanical model of the Reissner-Nordström black hole", Physical Review D, 57, 4899–4916 (1998).
[24] Y. C. Ong and M. R. R. Good, "The quantum atmosphere of Reissner-Nordström black holes", Physical Review Research, 2, 033322 (2020).
[25] S. M. Carroll, M. C. Johnson and L. Randall, "Extremal limits and black hole entropy", Journal of High Energy Physics, 11, 109 (2009).